

The Cyanobacterial NAD Kinase Gene *sll1415* Is Required for Photoheterotrophic Growth and Cellular Redox Homeostasis in *Synechocystis* sp. Strain PCC 6803

Hong Gao and Xudong Xu

State Key Laboratory of Freshwater Ecology and Biotechnology, Institute of Hydrobiology, Chinese Academy of Sciences, Wuhan, Hubei, China

NAD kinase (NADK), which phosphorylates NAD to NADP, is one of the key enzymes regulating the cellular NADP(H) level. In *Synechocystis* sp. strain PCC 6803, *slr0400* and *sll1415* were shown to encode NAD kinases. The NADP(H) pool in the cyanobacterium was remarkably reduced by an *sll1415*-null mutation but slightly reduced by an *slr0400*-null mutation. The reduction of the NADP(H) level in the *sll1415* mutant led to a significant accumulation of glucose-6-phosphate and a loss of photoheterotrophic growth. As the primary NADK gene, *sll1415* was found to inhibit the transcription of genes involved in redox homeostasis and to exert stronger effects on methyl viologen tolerance than *slr0400*.

NAD kinase (NADK) (EC 2.7.1.23) is the enzyme that catalyzes the phosphorylation of NAD to NADP in the presence of a phosphoryl donor, ATP or poly(P) (17). It is the key enzyme that regulates the cellular NADP(H) level and, consequently, NADPH-dependent reductive biosynthetic pathways, defense against oxidative stresses, and detoxification reactions (1). NAD kinases from different organisms can form homomultimers (2-mer, 4-mer, 6-mer, and 8-mer), and the homomultimer structure is important for creating NAD- and ATP-binding sites (17). The crystal structures of several NAD kinases in apo and/or holo forms have been solved (10, 21–23, 26). In combination with site-directed mutagenesis studies, the protein structures indicate that at least three highly conserved motifs, GGDG, NE/D, and conserved region II, are involved in the formation of the NAD-binding site (22, 27), which overlaps with the ATP-binding site (21). The Asp residue of the GGDG motif may also play a role in abstracting a proton from NAD to activate the phosphoacceptor (26).

The first NADK gene identified was that of *Mycobacterium tuberculosis* (15). Afterwards, NADK genes were identified in many other microorganisms, plants, and animals. In microorganisms with a single NADK gene in the genome, such as *Mycobacterium tuberculosis* and *Salmonella enterica*, the inactivation of that gene is lethal (11, 28). In *Saccharomyces cerevisiae* (yeast) (19, 24, 29, 32) and *Arabidopsis thaliana* (plant) (2, 3, 6, 33), which possess three NADK genes per genome, the mutation of one of the NADK genes is not lethal; however, some of these NADK gene mutants showed increased sensitivity to oxidative stresses (2, 6, 19, 29), slow growth in a low-iron medium (29), defects in the biosynthesis of chlorophyll (6) or enzymes containing the Fe-S cluster (24), and other abnormal physiological phenotypes (32, 33). Certain NADK genes are upregulated by copper-, H₂O₂-, or irradiation-induced oxidative stresses (2, 32). In *Methanococcus jannaschii* (archaeon), NADK is fused with an NADP phosphatase, and the bifunctional NADK/NADPase is involved in maintaining a suitable balance of the cellular NAD/NADP concentration (16).

Cyanobacteria are oxygenic photosynthetic bacteria that possess photosystems I and II. They are widely distributed in the ocean and inland water bodies and on soil and rock surfaces (5). While most cyanobacteria use CO₂ as the sole carbon source, a

small number of species can grow heterotrophically on mono- or disaccharides. In cyanobacteria, NADPH is generated as a consequence of the photosynthetic electron transfer to NADP⁺ through ferredoxin or reactions catalyzed by NADP-dependent dehydrogenases (13). *Synechocystis* sp. strain PCC 6803, a unicellular cyanobacterium, can grow on either CO₂ (autotrophically) or glucose (heterotrophically) or on both (mixotrophically). Its utilization of glucose involves glucose-6-phosphate (G6P) dehydrogenase and 6-phosphogluconate (6PG) dehydrogenase; both are NADP-dependent dehydrogenases (30). Like many other cyanobacteria, *Synechocystis* sp. PCC 6803 possesses two predicted NADK genes. In this study, we found that *sll1415*, as the primary NADK-encoding gene, is required for the utilization of glucose and inhibits the expressions of *sll1621*, a type II peroxiredoxin gene, and *slr1843*, the G6P dehydrogenase gene in *Synechocystis* sp. PCC 6803.

MATERIALS AND METHODS

Strains, culture conditions, and transformation. Glucose-tolerant *Synechocystis* sp. strain PCC 6803 used in this study was obtained from J. Zhao of Beijing University. *Synechocystis* cells were grown in BG11 medium on a shaker (120 rpm) at 30°C with a photosynthetic photon flux density of 30 μE m⁻² s⁻¹. For mixotrophic growth, a final concentration of 5 mM glucose was added to the medium. For photoheterotrophic growth, a final concentration of 5 μM 3-(3,4-dichlorophenyl)-1,1-dimethylurea (DCMU) and 5 mM glucose were added to the medium. Kanamycin (10 μg ml⁻¹), spectinomycin (10 μg ml⁻¹), or erythromycin (5 μg ml⁻¹) was added to the medium as required.

The transformation of *Synechocystis* sp. PCC 6803 was performed as described previously (36). The complete segregation of the mutants was confirmed by PCR using primers. The *Synechocystis* strains and primers used are listed in Table 1.

Received 23 July 2011 Accepted 24 October 2011

Published ahead of print 4 November 2011

Address correspondence to Xudong Xu, xux@ihb.ac.cn.

Supplemental material for this article may be found at <http://jb.asm.org/>.

Copyright © 2012, American Society for Microbiology. All Rights Reserved.

doi:10.1128/JB.05873-11

TABLE 1 *Synechocystis* strains, plasmids, and primers

Strain, plasmid, or primer	Derivation, relevant characteristic(s), and/or sequence (5'→3') (source or reference[s]) ^a
<i>Synechocystis</i> strains	
WT	Wild type of <i>Synechocystis</i> sp. PCC 6803 (J. Zhao, Beijing University/Institute of Hydrobiology)
DRHB787	Em ^r <i>sll1415::C.E1</i> ; <i>Synechocystis</i> chromosomal bp 1602611–1603093 within <i>sll1415</i> replaced by C.E1
DRHB2968	Sp ^r ; Ω-P _{petE} - <i>sll1415</i> integrated into the EcoRI site of <i>slr0168</i> , a neutral platform in the genome of <i>Synechocystis</i> sp. PCC 6803, to enhance the expression of <i>sll1415</i>
DRHB2970	Km ^r <i>slr0400::C.K2</i> ; C.K2 inserted into the BamHI site of <i>slr0400</i>
DRHB3129	Sp ^r ; Ω-P _{petE} - <i>slr0400</i> integrated into the EcoRI site of <i>slr0168</i> , a neutral platform in the genome of <i>Synechocystis</i> sp. PCC 6803, to enhance the expression of <i>slr0400</i>
DRHB787/DRHB2968	Em ^r Sp ^r ; Ω-P _{petE} - <i>sll1415</i> integrated into the EcoRI site of <i>slr0168</i> in DRHB787 to complement the <i>sll1415::C.E1</i> mutation
DRHB2970/DRHB3129	Km ^r Sp ^r ; Ω-P _{petE} - <i>slr0400</i> integrated into the EcoRI site of <i>slr0168</i> in DRHB2970 to complement the <i>slr0400::C.K2</i> mutation
Plasmids^b	
pHB518	Cm ^r Em ^r Km ^r ; T-cloning vector (37)
pHB576	Cm ^r Sp ^r ; T-cloning vector (37)
pHB729	Em ^r Km ^r ; PCR fragment containing the 5' region of <i>sll1415</i> amplified with primers gp189-7 and gp189-8 and cloned into pHB518
pHB762	Sp ^r ; PCR fragment containing 3' region of <i>sll1415</i> amplified with primers gp189-9 and gp189-10 and cloned into pHB576
pHB787	Em ^r Km ^r Sp ^r ; the 5' region of <i>sll1415</i> flanking kanamycin and erythromycin was excised with Sse8387I from pHB729 and cloned into the same site of pHB762
pHB1524	Ap ^r Sp ^r ; plasmid containing Ω-P _{petE} (9)
pHB2970	Ap ^r Km ^r ; PCR fragment containing <i>slr0400</i> and flanking regions amplified with primers slr0400-1 and slr0400-2, digested with BamHI, ligated with a C.K cassette excised with BamHI from pRL446, reamplified by PCR using primers slr0400-1 and slr0400-2, separated and purified on gel, and cloned into pMD18-T
pHB2944	Ap ^r ; PCR fragment containing the ORF of <i>sll1415</i> amplified with primers sll1415-1 and sll1415-2 and cloned into pMD18-T
pHB2952	Ap ^r Sp ^r ; Ω-P _{petE} excised from pHB1524 with SalI and BamHI, blunted with T4 DNA polymerase, and cloned into XbaI-cut and T4 DNA polymerase-blunted pHB2944 to form Ω-P _{petE} - <i>sll1415</i>
pHB2960	Ap ^r ; PCR fragment containing <i>sll1415</i> amplified with primers sll1415e-1 and sll1415e-2 and cloned into pMD18-T
pHB2966	Ap ^r ; <i>sll1415</i> excised with NdeI and XhoI from pHB2960 and cloned between the NdeI and XhoI sites of pET21b
pHB2968	Ap ^r Sp ^r ; Ω-P _{petE} - <i>sll1415</i> excised from pHB2952 with PvuII cloned into EcoRI-cut and T4 DNA polymerase-blunted pKW1188
pHB3043	Ap ^r ; PCR fragment containing <i>slr0400</i> amplified with primers slr0400e-1 and slr0400e-2 and cloned into pMD18-T
pHB3049	Ap ^r ; <i>slr0400</i> excised with NdeI and XhoI from pHB3049 and cloned between the NdeI and XhoI sites of pET21b
pHB3119	Ap ^r ; PCR fragment containing ORF of <i>slr0400</i> amplified with primers slr0400e-3 and slr0400e-4 and cloned into pMD18-T
pHB3128	Ap ^r Sp ^r ; Ω-P _{petE} fragment excised with SalI and BamHI from pHB1524, blunted with T4 DNA polymerase, and cloned into the XbaI-cut and T4 DNA polymerase-blunted pHB3119
pHB3129	Ap ^r Sp ^r ; Ω-P _{petE} - <i>slr0400</i> excised from pHB3128 with PvuII and cloned into EcoRI-cut and T4 DNA polymerase-blunted pKW1188
pET21b	Ap ^r ; overexpression vector (Novagen, EMD Chemicals Inc.)
pKW1188	Ap ^r Km ^r ; plasmid bearing the neutral integrative platform for <i>Synechocystis</i> sp. PCC 6803 (9, 36)
pMD18-T	Ap ^r ; T-cloning vector (Takara, Japan)
pRL446	Ap ^r Km ^r ; plasmid containing kanamycin resistance cassette C.K2 (7)
Primers	
gp189-7	GACGGCAACTCGATCAGCAA
gp189-8	GTGGATGGCCCATCGAGCAG
gp189-9	ACCATTCGATGTGTTCCAGG
gp189-10	GGTCAAGGATTAGACCTGT
sll1415e-1	GCATATGGTGGAACTGAAACAGGTG
sll1415e-2	CCTCGAGATTGACCTTGTGTTACC
sll1415-1	GGTGTGGAAGATGCCGCCG
sll1415-2	TCCTTGCCCGCACGAAATCT
sll1415rt-1 ^c	AGGGAAGTGAAGCTAGGGG
sll1415rt-3 ^c	GGTTGAGACGGTCCCACACT
slr0400-1	GTGTGGCCCGTAAAACCTATCC
slr0400-2	CACCCGGTCTTCTGGCAACAC
slr0400e-1	GCATATGGTGCCAAAAGTCGGCATC
slr0400e-2	CCTCGAGTGGCAACTCCACCGATGTTGG
slr0400e-3	CTAGGATCTCGCCCCTGTG
slr0400e-4	GGCGGCGGGAATAGCAGGGT
slr0400rt-1 ^c	CAGAGTGGGTTACAGTGGCG
slr0400rt-2 ^c	GTCAACAGGGGGATGCCGAG

Continued on following page

TABLE 1 (Continued)

Strain, plasmid, or primer	Derivation, relevant characteristic(s), and/or sequence (5'→3') (source or reference[s]) ^a
sll1621rt-1 ^c	CCCAAGTGTAGTGTTCAAAACCCG
sll1621rt-2 ^c	AACAACCTGCTCGTAGCGGGGCAA
slr1843rt-1 ^c	GTGCCAGCCATCTACCAAAT
slr1843rt-2 ^c	GGGCATCCATATTGCCAGA
rnpBrT-1 ^c	CAGGGAATCTGAGGAAAGTCC
rnpBrT-2 ^c	CTTACCGCACCTTTGCACCT

^a Abbreviations: Ap, ampicillin; Em, erythromycin; Km, kanamycin; Sp, spectinomycin; Cm, chloramphenicol; ORF, open reading frame; WT, wild type. Designations with DRHB refer to a product of double homologous recombination between a pHB plasmid and the *Synechocystis* sp. genome.

^b Unless stated otherwise, the template for PCR was *Synechocystis* sp. genomic DNA.

^c Primers used for qRT-PCR.

Plasmid construction. Molecular manipulations were performed according to standard protocols. Molecular tool enzymes were used according to instructions provided by the manufacturers. PCR fragments cloned into pMD18-T (Takara) were confirmed by sequencing. Details of plasmid construction processes and primers used are described in Table 1.

Plasmid pHB787 was used to inactivate *sll1415* in *Synechocystis* sp. PCC 6803, pHB2970 was used to inactivate *slr0400*, pHB2968 was used to complement the *sll1415* mutant, pHB3129 was used to complement the *slr0400* mutant, pHB2966 was used to express recombinant Sll1415 in *Escherichia coli*, and pHB3049 was used to express recombinant Slr0400 in *E. coli*.

Expression of *Synechocystis* NADK genes in *Escherichia coli*. *E. coli* BL21(DE3) cells were transformed with plasmids pET21b, pHB2966, and pHB3049, respectively. *E. coli* cells were grown in LB medium supplemented with 50 μg/ml ampicillin and induced with 0.5 μM isopropyl-β-D-thiogalactopyranoside (IPTG) for 10 h at 30°C.

Assays of NAD kinase activity. *E. coli* or cyanobacterial cells were harvested by centrifugation at 4°C, washed twice with 50 mM Tris-HCl (pH 7.5), and resuspended in the same buffer. Cells were broken by sonication, cell debris was removed by centrifugation at 4°C, and the supernatants were used for NAD kinase assays. NAD kinase assays were performed according to a previously described two-step procedure (11), with modifications. The reaction mixture used in the first step included 5.0 mM NAD, 10 mM MgCl₂, 10 mM ATP, and 100 mM Tris-Cl (pH 7.5) in

a total volume of 200 μl. Reactions were initiated by the addition of 10 μl of the crude enzyme extracts to the mixture, allowed to proceed at 30°C for 30 min, and stopped by heating at 100°C for 90 s, followed by centrifugation to remove denatured proteins. The NADP⁺ produced in the first step was reduced to NADPH and quantified by determining the absorbance at 340 nm. The reduction was achieved by the addition of glucose-6-phosphate to a final concentration of 10 mM and 2 units of yeast glucose-6-phosphate dehydrogenase. One unit of enzyme activity was defined as nmol NADP(H) produced in 1 h at 30°C, and the specific activity was expressed in U · mg protein⁻¹ for *E. coli* cells or U · mg chlorophyll *a* (Chl *a*)⁻¹ for cyanobacterial cells. The concentration of the protein was determined as described previously by Bradford (4). Chl *a* was extracted with methanol and measured as described previously by Lichtenthaler (20).

Measurements of G6P and 6PG. The levels of G6P (glucose-6-phosphate) and 6PG (6-phosphogluconate) were determined as described previously (12), with modifications. The supernatants of cyanobacterial lysates were boiled for 10 min to inactivate enzymes in the extracts and centrifuged to remove denatured proteins. The level of G6P was determined by measuring the increase of the A₃₄₀ of the reaction mixture (0.2 ml) containing 0.02 ml of heat-treated extracts, 50 mM Tris-HCl (pH 7.4), 10 mM MgCl₂, 0.7 mM NADP, and 0.5 U/ml G6P dehydrogenase. The level of 6PG was determined by using the same procedure

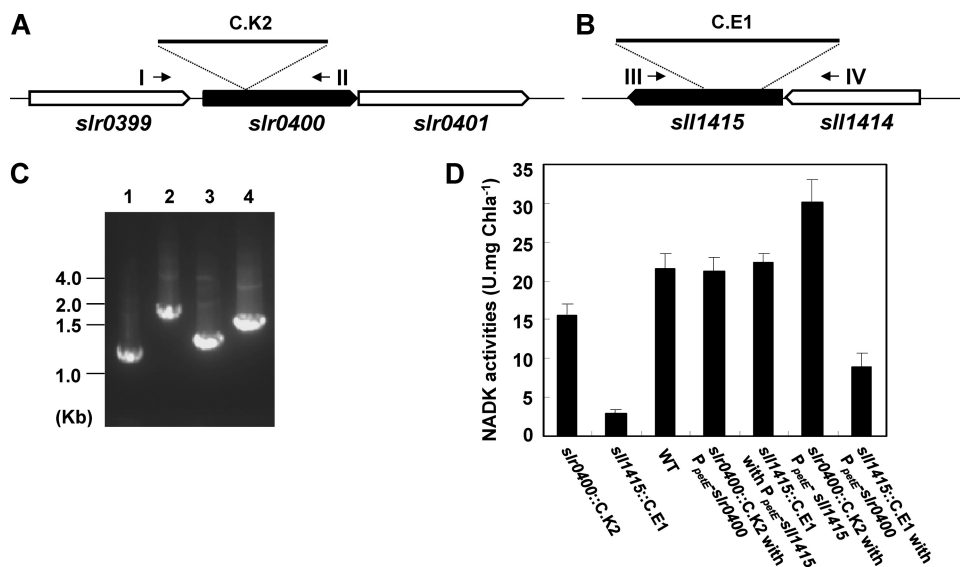


FIG 1 *sll1415*::C.E1 and *slr0400*::C.K2 mutants of *Synechocystis* sp. PCC 6803. (A) The *slr0400* region in the *slr0400*::C.K2 mutant. (B) The *sll1415* region in the *sll1415*::C.E1 mutant. (C) PCR examination showing the complete segregation of the *slr0400* mutant (lane 2) and the *sll1415* mutant (lane 4) compared to the wild-type strain (lanes 1 and 3), using primer pairs slr0400-1/sl0400-2 (I/II in A) and gp189-10/gp189-7 (III/IV in B), respectively. (D) NAD kinase activities of cyanobacterial strains.

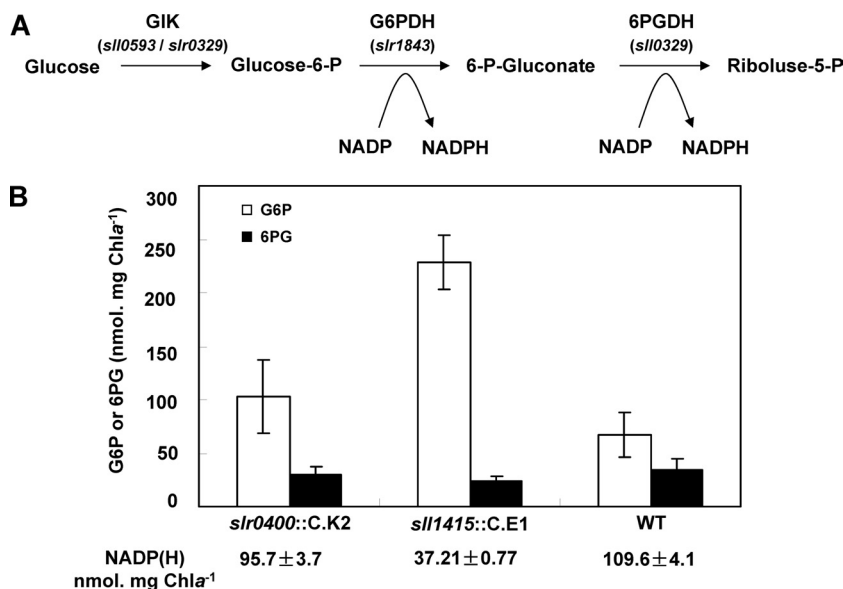


FIG 2 Accumulation of G6P in NADK mutants. (A) Reactions transforming glucose to ribulose-5-phosphate. GIK, glucokinase; G6PDH, glucose-6-phosphate dehydrogenase; 6PGDH, 6-phosphogluconate dehydrogenase. Encoding genes are indicated in parentheses. (B) G6P (empty bars) and 6PG (solid bars) levels in *Synechocystis* strains. The values represent means \pm standard deviations (SD) from three independent experiments.

except that 6PG dehydrogenase (0.025 U ml^{-1}) was used instead of G6P dehydrogenase.

Measurements of NADP(H). NADP and NADPH levels were determined by using high-performance liquid chromatography (HPLC) as described previously (21, 25), with modifications. Cyanobacterial cells were harvested by centrifugation at 4°C , resuspended with $200 \mu\text{l}$ of 0.5 M KOH , and propelled through a 23-gauge needle on a 1-ml syringe. After incubation on ice for 5 min, the extracts were neutralized with $100 \mu\text{l}$ of $1 \text{ M H}_3\text{PO}_4$. The supernatant was recovered by centrifugation at $12,000 \times g$ at 4°C for 5 min and filtered with a 5-kDa-cutoff filter (Millipore). The nucleotides in the filtrates were immediately separated by using a reverse-phase ion-pairing HPLC instrument (LC-20A; Shimada, Japan) equipped with an SPD-20A photodiode array detector (Shimadzu, Japan). NADP and NADPH were quantified based on the use of standards.

qRT-PCR. Total RNA was extracted from cells by using TRIzol reagent (Invitrogen), treated with RNase-free DNase I (Promega, Madison, WI), and reverse transcribed with the PrimeScript reverse transcription system (Takara, Dalian, China) according to the manufacturer's instructions. Quantitative real-time PCR (qRT-PCR) was conducted by using an ABI StepOne PCR system (Applied Biosystems) with a reaction mixture of $20 \mu\text{l}$ containing $0.3 \mu\text{M}$ each primer, $10 \mu\text{l}$ of SYBR Premix DimerEraser PCR master mix ($2\times$), $0.4 \mu\text{l}$ ROX reference dye ($50\times$) (Takara, Dalian, China), and $2 \mu\text{l}$ of template cDNA (100 ng). qRT-PCR was carried out with the following steps: an initial denaturation step at 95°C for 1 min followed by 40 cycles of 95°C for 5 s, 60°C for 30 s, and 72°C for 31 s. All samples were tested in triplicate, and a no-template control was included for each run. The relative abundance of each transcript was calculated from the standard curve with software provided by the manufacturer. *rnpB* (RNase P subunit B) (35) was used as the internal control. The primers for *sll1415*, *slr0400*, *sll1621*, *slr1843*, and *rnpB* are listed in Table 1. Two independent experiments were performed, which showed consistent results.

Phylogenetic analysis of NADKs. NADK amino acid sequences were retrieved from Cyanobase (<http://genome.kazusa.or.jp/cyanobase/>) and the NCBI GenBank database (<http://www.ncbi.nlm.nih.gov/protein/>). ClustalW and Mega 4 (http://www.ch.embnet.org/software/BOX_form.html) were employed for the phylogenetic analysis. A neighbor-joining (NJ) tree based on 1,000 bootstrap replicates was constructed.

RESULTS AND DISCUSSION

***slr0400* and *sll1415* are NADK genes in *Synechocystis* sp. PCC 6803.** In *Synechocystis* sp. PCC 6803, *slr0400* (chromosomal bp 2149333 to 2150250) and *sll1415* (chromosomal bp 1602482 to 1603405) are predicted to encode NADKs. All conserved motifs of NADKs, including the motifs GGDG, NE/D, and conserved region II, are found in their deduced amino acid sequences (see Fig. S1 in the supplemental material). To test the NADK activities of the encoded products, we expressed these two genes from the T7 promoter in *E. coli*. The expressions of *slr0400* and *sll1415* increased the NADK activity in the crude cell extracts of *E. coli* BL21(DE3) from $3.1 \pm 1.2 \text{ U} \cdot \text{mg protein}^{-1}$ (pET21b) to $8.2 \pm 1.8 \text{ U} \cdot \text{mg protein}^{-1}$ (pHB3049) and $113.6 \pm 5.5 \text{ U} \cdot \text{mg protein}^{-1}$ (pHB2966), respectively. *E. coli* cells expressing *slr0400* produced an extra lower band ($\sim 31 \text{ kDa}$) in addition to the one of the expected size ($\sim 34 \text{ kDa}$) (see Fig. S2 in the supplemental material), and recombinant Slr0400 appeared to possess lower levels of NADK activity than recombinant Sll1415.

On the other hand, we examined their effects on the NADK activity of *Synechocystis* sp. PCC 6803. Two mutants, *slr0400::C.K2* (DRHB2970 in Table 1) and *sll1415::C.E1* (DRHB787 in Table 1), were generated by the insertion of antibiotic resistance cassettes

TABLE 2 Growth rates of *Synechocystis* strains

Strain	Mean growth rate (no. of doublings $\cdot \text{day}^{-1}$) \pm SD		
	Photoautotrophic	Photoheterotrophic	Mixotrophic
<i>slr0400::C.K2</i>	1.09 ± 0.02	1.19 ± 0.13	1.32 ± 0.06
<i>sll1415::C.E1</i>	1.10 ± 0.15	0.15 ± 0.05	1.24 ± 0.13
<i>slr0400::C.K2</i> complemented	1.10 ± 0.08	1.20 ± 0.04	1.22 ± 0.08
<i>sll1415::C.E1</i> complemented	1.14 ± 0.12	1.10 ± 0.08	1.31 ± 0.06
Wild type	1.13 ± 0.09	1.12 ± 0.06	1.33 ± 0.04

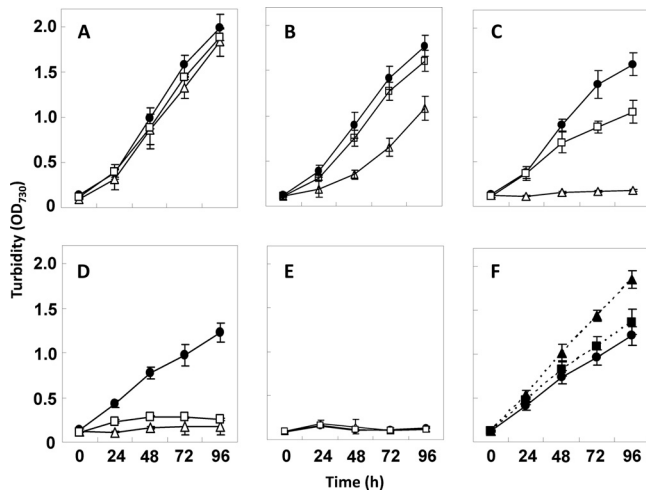


FIG 3 Sensitivity of *Synechocystis* strains to methyl viologen (MV) under autotrophic growth conditions. Cells were grown in BG11 medium supplemented with MV at 0 μM (A), 0.5 μM (B), 0.75 μM (C), 1.0 μM (D and F), or 2.0 μM (E) under illumination at a photon flux density of 30 $\mu\text{E m}^{-2} \text{s}^{-1}$. Solid circles, wild-type strain; empty squares, the *slr0400*::C.K2 mutant (DRHB2970); empty triangles, the *sll1415*::C.E1 mutant (DRHB787); solid squares, the *slr0400*-overexpressing strain (DRHB3129); solid triangles, the *sll1415*-overexpressing strain (DRHB2968). OD₇₃₀, optical density at 730 nm.

into these genes (Fig. 1A to C). The NADK activity of the *sll1415*::C.E1 mutant was reduced to about 14% of that of the wild type, while the *slr0400*::C.K2 mutant retained about 77% of the NADK activity compared to that of the wild type. We also complemented the mutants with *slr0400* or *sll1415*. The DNA fragment containing only *slr0400* (chromosomal bp 2149317 to 2150274) or *sll1415* (chromosomal bp 1602336 to 1603446) was cloned downstream of the P_{petE} promoter and integrated into a neutral platform (9) in the genome. The complementation of the *slr0400*::C.K2 mutant with P_{petE} -*slr0400*, or the complementation of the *sll1415*::C.E1 mutant with P_{petE} -*sll1415*, completely restored the NADK activities in the mutants to the wild-type level (Fig. 1D). The complementation experiment indicated that the phenotype of each mutant was not due to a second mutation or a polar effect. The cross-complementation of the *slr0400*::C.K2 mutant with P_{petE} -*sll1415* resulted in higher levels of NADK activity, and the cross-

complementation of the *sll1415*::C.E1 mutant with P_{petE} -*slr0400* resulted in lower levels of NADK activity, than the wild type level. In combination with the activities of recombinant Slr0400 and Sll1415 in *E. coli*, this result suggested that Slr0400 should contribute less than Sll1415 to the cellular NADK activity in the cyanobacterium. Although each of the NADK genes was readily inactivated in *Synechocystis* sp. PCC 6803, the inactivation of *sll1415* in the *slr0400*::C.K2 mutant or the inactivation of *slr0400* in the *sll1415*::C.E1 mutant could not be completely segregated, suggesting that NAD kinase activity was essential for the growth of the cyanobacterium.

***sll1415* is required for photoheterotrophic growth.** The utilization of glucose in *Synechocystis* sp. PCC 6803 involves the conversion of glucose to glucose-6-phosphate (G6P) and, consequently, to 6-phosphogluconate (6PG) and to ribulose-5-phosphate (R5P). Under mixotrophic conditions, the NADP(H) level in *Synechocystis* sp. PCC 6803 was $109.6 \pm 4.1 \text{ nmol} \cdot \text{mg Chl } a^{-1}$, while that in the *sll1415* mutant decreased to $37.2 \pm 0.8 \text{ nmol} \cdot \text{mg Chl } a^{-1}$, and that in the *slr0400* mutant was only slightly reduced ($95.7 \pm 3.9 \text{ nmol} \cdot \text{mg Chl } a^{-1}$). The reduction in the NADP(H) pool may directly limit NADP-dependent reactions. We measured cellular levels of G6P and 6PG (Fig. 2). In the *sll1415* mutant, G6P was accumulated to about 3.5-fold of the wild-type level. In the *slr0400* mutant, the G6P level also showed a slight increase. The accumulation of G6P should be an indication of the limited conversion of G6P to 6PG. The 6PG level, however, was determined by the rates of generation from G6P and conversion to R5P (Fig. 2), both limited by the NADP level. Therefore, the 6PG level was not reduced in the *sll1415* mutant at amplitude, in accordance with the accumulation of G6P.

We used DCMU to inhibit photosynthesis in *Synechocystis* sp. PCC 6803 so that the growth of these strains was based on the utilization of glucose as the sole carbon source. Under our conditions, DCMU at 5 μM could completely inhibit the photoautotrophic growth of the cyanobacterium. Under photoheterotrophic conditions, the *sll1415*::C.E1 mutant rather than the *slr0400*::C.K2 mutant showed a greatly reduced growth rate relative to that of the wild type (Table 2). A complementation of the *sll1415* mutant restored photoheterotrophic growth. Under autotrophic or mixotrophic conditions, both mutants grew like the

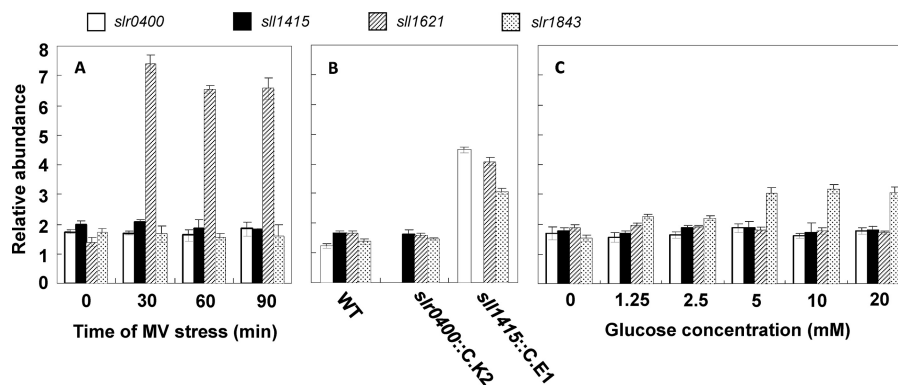


FIG 4 Evaluation of gene expression by qRT-PCR. (A) mRNA levels of *slr0400*, *sll1415*, and *sll1621* under conditions of MV-induced oxidative stress. (B) mRNA levels of *slr0400*, *sll1415*, *sll1621*, and *slr1843* in the wild type and the NADK mutants. (C) mRNA levels of *slr0400*, *sll1415*, *sll1621*, and *slr1843* in medium supplemented with glucose at different concentrations.

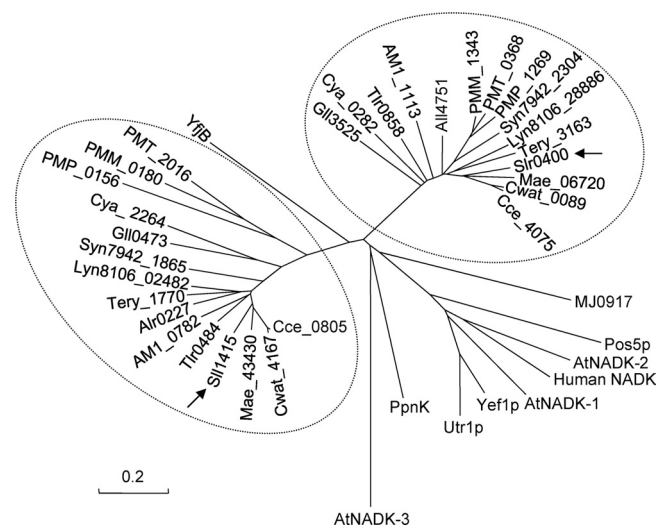


FIG 5 Dendrogram of cyanobacterial NAD kinase homologues. Arrows point to Sll1415 (GenBank accession number NP_441342) and Slr0400 (accession number NP_441852) from *Synechocystis* sp. PCC 6803. Alr0227 (accession number NP_484271) and All4751 (accession number NP_488791) are from *Anabaena/Nostoc* sp. strain PCC 7120; Tll0858 (accession number NP_681648) and Tlr0484 (accession number NP_681274) are from *Thermosynechococcus elongatus* BP-1; Gll0473 (accession number NP_923419) and Gll3525 (accession number NP_926471) are from *Gloeobacter violaceus* PCC 7421; Cya_2264 (accession number YP_475664) and Cya_0282 (accession number YP_473767) are from *Synechococcus* sp. strain JA-3-3Ab; Cce_4075 (accession number YP_001805489) and Cce_0805 (accession number YP_001802222) are from *Cyanothece* sp. strain ATCC 51142; Mae_06720 (accession number YP_001655686) and Mae_43430 (accession number YP_001659357) are from *Microcystis aeruginosa* NIES-843; AM1_1113 (accession number YP_001515466) and AM1_0782 (accession number YP_001515140) are from *Acarochloris marina* MBIC11017; PMT_2016 (accession number CAE22190) and PMT_0368 (accession number CAE20543) are from *Prochlorococcus marinus* MIT9313; Syn7942_2304 (accession number YP_401321) and Syn7942_1865 (accession number YP_400882) are from *Synechococcus elongatus* PCC 7942; PMP_0156 (accession number NP_892277) and PMP_1269 (accession number NP_893386) are from *Prochlorococcus marinus* subsp. *pastoris* strain CCMP1986; PMM_0180 (accession number NP_874574) and PMM_1343 (accession number NP_875734) are from *Prochlorococcus marinus* subsp. *marinus* strain CCMP1375; Lyn8106_02482 (accession number ZP_01622166) and Lyn8106_28886 (accession number ZP_01621456) are from *Lyngbya* sp. strain PCC 8106; Tery_1770 (accession number YP_721503) and Tery_3163 (accession number YP_722764) are from *Trichodesmium erythraeum* IMS101; Cwat_4167 (accession number ZP_00515774) and Cwat_0089 (accession number ZP_00519346) are from *Crocospheara watsonii* WH 8501; MJ0917 (accession number NP_247912) is from *Methanocaldococcus jannaschii* DSM 2661; YfjB (accession number NP_417105) is from *Escherichia coli* K-12; PpnK (accession number NP_216211) is from *Mycobacterium tuberculosis* H37Rv; Pos5p (accession number NP_015136), Utr1p (accession number NP_012583), and Yef1p (accession number NP_010873) are from *Saccharomyces cerevisiae*; AtNADK-1 (accession number NP_974347), AtNADK-2 (accession number NP_177980), and AtNADK-3 (accession number NP_564145) are from *Arabidopsis thaliana*; and human NADK (accession number NP_075394) is from *Homo sapiens*. The bar indicates 0.2 substitutions per site.

wild type. These results indicated that *sll1415* is required for the photoheterotrophic growth of the cyanobacterium.

***sll1415* affects cellular redox homeostasis.** In cyanobacteria and plants, methyl viologen (MV) can efficiently accept the electron from photosystem I and reduce O_2 into O_2^- , which damages macromolecules and membranes. Due to the superoxide-scavenging systems, *Synechocystis* sp. PCC 6803 can tolerate a relatively low concentration (for example, $0.5 \mu M$) of methyl violo-

gen (34). The scavenging of superoxide, however, eventually depends on the reducing equivalents, such as NADPH, in cells (14). We compared the growths of the NADK gene mutants and the wild-type strain in BG11 medium with different concentrations of MV (Fig. 3). These strains showed no difference in medium without MV. With the increase in the level of MV, the growths of these strains ceased at different concentrations: the *sll1415* mutant showed no growth at $0.75 \mu M$, and the *slr0400* mutant showed no growth at $1.0 \mu M$, while the wild type showed no growth at $2.0 \mu M$. On the other hand, the supplementation of P_{petE} -*sll1415* or P_{petE} -*slr0400* to the wild-type genome to enhance their expression increased the tolerance to MV, as shown by the growth at $1 \mu M$ MV (Fig. 3).

Because *sll1415* and *slr0400* affect the sensitivity to MV, we wondered if they are inducible in response to MV-induced oxidative stress. The transcript abundances of these two genes and *sll1621*, which was used as the positive control, were evaluated by qRT-PCR. *sll1621*, as a type II peroxiredoxin gene, is inducible by MV and is involved in the cellular defense against oxidative stress (18, 31). As shown in Fig. 4A, neither of the two NADK genes was induced by MV, while *sll1621* showed a rapid response. On the other hand, we wondered if genes that are responsive to oxidative stress are induced by the NADK gene mutations. In addition to *sll1621*, we used *slr1843*, the G6P dehydrogenase gene, as an indicator. *slr1843* is involved in oxidative defense due to its role in the generation of NADPH. The inactivation of *sll1415* significantly increased the expression levels of *sll1621* and *slr1843*, suggesting that the cellular redox homeostasis was disturbed (Fig. 4B). Also, *slr0400* showed significantly higher expression levels in the *sll1415* mutant than in the wild type. The increased expression level of *slr0400* was probably a strategy to compensate for the inactivation of *sll1415*. When glucose was supplemented at concentrations of 5 mM and higher, *slr1843*, the gene required for the utilization of glucose, showed increased expression at the mRNA level (Fig. 4C). Relating to heterotrophic growth, the two NADK genes, however, showed no response to the increase in the amount of glucose in the medium. The transcription of *sll1621* also remained unchanged.

***sll1415* and probably its homologues in other cyanobacteria are the primary NADK genes.** Based on the following four lines of evidence, we conclude that *sll1415* is the primary NADK gene in *Synechocystis* sp. PCC 6803: (i) the *sll1415*-null mutation affected NADK activity and the NADP(H) level more strongly than did the *slr0400*-null mutation; (ii) *sll1415* rather than *slr0400* was required for photoheterotrophic growth; (iii) *sll1415* played a more important role than *slr0400* in MV tolerance; and (iv) *sll1415* rather than *slr0400* affected the expression of oxidative stress-responsive genes. We noticed that the effects of NADK genes on the NADP(H) pool, photoheterotrophic growth, MV tolerance, and the expressions of other genes were not proportional to each other. This could be explained by the different responses of these physiological processes to the availability of NADP(H) in cells. Certain processes may be activated only when the cellular NADP(H) level is over a certain threshold.

A Blast search of cyanobacterial genomes available in the NCBI GenBank database showed that all of them possess two predicted NAD kinase genes, each grouped with *sll1415* or *slr0400*, as shown in the dendrogram of NADK homologues in Fig. 5. The expression of the two predicted NADK genes from *Anabaena* sp. strain PCC 7120 also increased NADK activities in *E. coli* (data not shown). It is reasonable to hypothesize that the homologues of

slr1415 in other cyanobacteria are also the primary NADK genes. However, it remains to be answered why all these cyanobacterial species have two NADK genes, with one of them being the major player in the conversion of NAD to NADP. The coexistence of two encoding genes for the same enzyme activity may imply functional divergence. For example, the two glycogen phosphorylase genes in *Synechocystis* sp. PCC 6803 actually play different roles in high-temperature tolerance and glycogen utilization (8). The additional physiological function, if any, of *slr0400* in the cyanobacterium awaits investigations.

ACKNOWLEDGMENTS

This research was supported by the National Natural Science Foundation of China (grant 30825003) and the State Key Basic Research Development Program of China (grant 2008CB418001).

REFERENCES

- Agledal L, Niere M, Ziegler M. 2009. The phosphate makes a difference: cellular functions of NADP. *Redox Rep.* 15:2–10.
- Berrin JG, et al. 2005. Stress induces the expression of AtNADK-1, a gene encoding a NAD(H) kinase in *Arabidopsis thaliana*. *Mol. Gen. Genet.* 273:10–19.
- Bieganowski P, Seidle HF, Wojcik M, Brenner C. 2006. Synthetic lethal and biochemical analyses of NAD and NADH kinases in *Saccharomyces cerevisiae* establish separation of cellular functions. *J. Biol. Chem.* 281:22439–22445.
- Bradford MM. 1976. A rapid and sensitive method for the quantitation of microgram quantities of protein utilizing the principle of protein-dye binding. *Anal. Biochem.* 72:248–254.
- Castenholz RW. 2001. Oxygenic photosynthetic bacteria, p 474–599. In Boone DR, Castenholz RW (ed), *Bergey's manual of systematic bacteriology*, 2nd ed. Springer-Verlag Publishing Company, Berlin, Germany.
- Chai MF, et al. 2005. NADK2, an *Arabidopsis* chloroplastic NAD kinase, plays a vital role in both chlorophyll synthesis and chloroplast protection. *Plant Mol. Biol.* 59:553–564.
- Elhai J, Wolk CP. 1988. A versatile class of positive-selection vectors based on the nonviability of palindrome-containing plasmids that allows the cloning into long polylinkers. *Gene* 68:119–138.
- Fu J, Xu X. 2006. Functional divergence of two *glgP* homologues in *Synechocystis* sp. PCC 6803. *FEMS Microbiol. Lett.* 260:201–209.
- Gao H, Xu X. 2009. Depletion of *Vipp1* in *Synechocystis* sp. PCC 6803 affects photosynthetic activity before the loss of thylakoid membranes. *FEMS Microbiol. Lett.* 292:63–70.
- Garavaglia S, Raffaelli N, Finaurini L, Magni G, Rizzi M. 2004. A novel fold revealed by *Mycobacterium tuberculosis* NAD kinase, a key allosteric enzyme in NADP biosynthesis. *J. Biol. Chem.* 279:40980–40986.
- Grose JH, Joss L, Velick SF, Roth JR. 2006. Evidence that feedback inhibition of NAD kinase controls responses to oxidative stress. *Proc. Natl. Sci. U. S. A.* 103:7601–7606.
- Hasan MR, Rahman M, Jaques S, Purwantini E, Daniels L. 2010. Glucose-6-phosphate accumulation in mycobacteria: implications for a novel F420-dependent anti-oxidant defense system. *J. Biol. Chem.* 285:19135–19144.
- Hurley JK, et al. 2002. Structure-function relationships in *Anabaena* ferredoxin/ferredoxin:NADP(+) reductase electron transfer: insights from site-directed mutagenesis, transient absorption spectroscopy and X-ray crystallography. *Biochim. Biophys. Acta* 1554:5–21.
- Jones DP. 2008. Radical-free biology of oxidative stress. *Am. J. Physiol. Cell Physiol.* 295:849–868.
- Kawai S, et al. 2000. Inorganic polyphosphate/ATP-NAD kinase of *Mycobacterium tuberculosis* H37Rv. *Biochem. Biophys. Res. Commun.* 276:57–63.
- Kawai S, Fukuda C, Mukai T, Murata K. 2005. MJ0917 in archaeon *Methanococcus jannaschii* is a novel NADP phosphatase/NAD kinase. *J. Biol. Chem.* 280:39200–39207.
- Kawai S, Murata K. 2008. Structure and function of NAD kinase and NADP phosphatase: key enzymes that regulate the intracellular balance of NAD(H) and NADP(H). *Biosci. Biotechnol. Biochem.* 72:919–930.
- Kobayashi M, et al. 2004. Response to oxidative stress involves a novel peroxiredoxin gene in the unicellular cyanobacterium *Synechocystis* sp. PCC 6803. *Plant Cell Physiol.* 45:290–299.
- Krems B, Charizanis C, Entian KD. 1995. Mutants of *Saccharomyces cerevisiae* sensitive to oxidative and osmotic stress. *Curr. Genet.* 27:427–434.
- Lichtenthaler HK. 1987. Chlorophylls and carotenoids, the pigments of photosynthetic biomembranes. *Methods Enzymol.* 148:350–382.
- Liu J, et al. 2005. Crystal structures of an NAD kinase from *Archaeoglobus fulgidus* in complex with ATP, NAD, or NADP. *J. Mol. Biol.* 354:289–303.
- Mori S, et al. 2005. NAD-binding mode and the significance of intersubunit contact revealed by the crystal structure of *Mycobacterium tuberculosis* NAD kinase-NAD complex. *Biochem. Biophys. Res. Commun.* 327:500–508.
- Oganesyan V, et al. 2005. Structure of a NAD kinase from *Thermotoga maritima* at 2.3 Å resolution. *Acta Crystallogr. Sect. F Struct. Biol. Cryst. Commun.* 61:640–646.
- Outten CE, Culotta VC. 2003. A novel NADH kinase is the mitochondrial source of NADPH in *Saccharomyces cerevisiae*. *EMBO J.* 9:2015–2024.
- Pollak N, Niere M, Ziegler M. 2007. NAD kinase levels control the NADPH concentration in human cells. *J. Biol. Chem.* 282:33562–33571.
- Poncet-Montange G, Assairi L, Arold S, Pochet S, Labesse G. 2007. NAD kinases use substrate-assisted catalysis for specific recognition of NAD. *J. Biol. Chem.* 282:33925–33934.
- Raffaelli N, et al. 2004. Characterization of *Mycobacterium tuberculosis* NAD kinase: functional analysis of the full length enzyme by site-directed mutagenesis. *Biochemistry* 43:7610–7617.
- Sasseti CM, Boyd DH, Rubin EJ. 2003. Genes required for mycobacterial growth defined by high density mutagenesis. *Mol. Microbiol.* 48:77–84.
- Shi F, Kawai S, Mori S, Kono E, Murata K. 2005. Identification of ATP-NADH kinase isozymes and their contribution to supply of NADP(H) in *Saccharomyces cerevisiae*. *FEBS J.* 272:3337–3349.
- Smith AJ. 1982. Modes of cyanobacterial carbon metabolism, p 47–85. In Carr NG, Whitton BA (ed), *The biology of cyanobacteria*. University of California Press, Berkeley, CA.
- Stork T, Michel KP, Pistorius EK, Dietz KJ. 2005. Bioinformatic analysis of the genomes of the cyanobacteria *Synechocystis* sp. PCC 6803 and *Synechococcus elongatus* PCC 7942 for the presence of peroxiredoxins and their transcript regulation under stress. *J. Exp. Bot.* 56:3193–3206.
- Strand MK, et al. 2003. POS5 gene of *Saccharomyces cerevisiae* encodes a mitochondrial NADH kinase required for stability of mitochondrial DNA. *Eukaryot. Cell* 2:809–820.
- Takahashi H, et al. 2006. Chloroplast NAD kinase is essential for energy transduction through the xanthophyll cycle in photosynthesis. *Plant Cell Physiol.* 47:1678–1682.
- Tichy M, Vermaas W. 1999. In vivo role of catalase-peroxidase in *Synechocystis* sp. strain PCC6803. *J. Bacteriol.* 181:1875–1882.
- Vioque A. 1992. Analysis of the gene encoding the RNA subunit of ribonuclease P from cyanobacteria. *Nucleic Acids Res.* 20:6331–6337.
- Williams JGK. 1988. Construction of specific mutations in photosystem II photosynthetic reaction center by genetic engineering methods in *Synechocystis* 6803. *Methods Enzymol.* 167:766–778.
- Zhang W, et al. 2007. A gene cluster that regulates both heterocyst differentiation and pattern formation in *Anabaena* sp. strain PCC 7120. *Mol. Microbiol.* 66:1429–1443.